HIV RNA dimerisation interference by antisense oligonucleotides targeted to the 5' UTR structural elements

José A. Reyes-Darias, Francisco J. Sánchez-Luque and Alfredo Berzal-Herranz*

Instituto de Parasitología y Biomedicina “López-Neyra” (IPBLN-CSIC),

Parque Tecnológico de Ciencias de la Salud,

Av. del Conocimiento s/n, Armilla, 18100 Granada, Spain.

Tel: +34 958 181 648

Fax: +34 958 181 632

*Correspondence should be addressed to:

Alfredo Berzal-Herranz

Instituto de Parasitología y Biomedicina “López-Neyra” (IPBLN-CSIC), Parque Tecnológico de Ciencias de la Salud, Av. del Conocimiento s/n, Armilla 18100, Granada, Spain.

Tel: +34 958 181 648; Fax: +34 958 181 632; E-mail: aberzalh@ipb.csic.es

Abstract

The HIV-1 genome consists of two identical RNA molecules non-covalently linked by their 5' unstranslatable regions (5'UTR). The high level of sequence and structural conservation of this region correlates with its important functional involvement in the viral cycle, making it an attractive target for antiviral treatments based on antisense technology. Ten unmodified DNA antisense oligonucleotides (ODNs) targeted against different conserved structural elements within the 5'UTR were assayed for their capacity to interfere with HIV-1 RNA dimerisation, inhibit gene expression, and prevent virus production in cell cultures. The results show that, in addition to the well-characterised dimerisation initiation site (DIS), targeting of the AUG-containing structural element may reflect its direct role in HIV-1 genomic RNA dimerisation *in vitro*. Similarly, blocking the 3' end sequences of the stem-loop domain containing the primer biding site interferes with RNA dimerisation. Targeting the apical portion of the TAR element, however, appears to promote dimerisation. ODNs targeted against the conserved polyadenylation signal [Poly(A)], the primer binding site (PBS), the major splicing donor (SD) or the major packaging signal (Psi), and AUG-containing structural elements led to a highly efficient inhibition of HIV-1 gene expression and virus production in cell culture. Together, these results support the idea that ODNs possess great potential as molecular tools for the functional characterisation of viral RNA structural domains. Moreover, the targeting of these domains leads to the potent inhibition of viral replication, underscoring the potential of conserved structural RNA elements as antiviral targets.

Keywords: HIV-1, RNA dimerisation, genomic RNA structural domains, antiviral antisense ODNs, anti-HIV targets.

1. Introduction

The genomes of RNA viruses are multifunctional molecules. In retroviruses, including human immunodeficiency virus type 1 (HIV-1), they function as both mRNA and genomic RNA (gRNA). Infective HIV-1 viral particles contain two identical, non-covalently linked gRNA molecules that bind in a process known as genomic RNA dimerisation (Paillart et al., 2004). It has been reported that RNA dimers are preferentially packaged over monomeric RNA genomes (Darlix et al., 1990; Fu and Rein, 1993). The dimeric state also facilitates template switching during reverse transcription, thus avoiding the problems that could be caused by any physical damage to one of the RNA monomers. It also favours recombination, increasing the genetic diversity and adaptability of retroviruses (Gotte et al., 1999). Electron microscopy studies of packaged retroviral gRNAs have revealed that the two RNA molecules attach to each other through the dimer linkage structure (DLS) in their 5' ends (Bender and Davidson, 1976; Hoglund et al., 1997). Using *in vitro*-transcribed short RNAs corresponding to various lengths of HIV-1 gRNA, it has been shown that the DLS includes the first 311 nucleotides of the HIV-1 5'UTR (Marquet et al., 1994). This 5'UTR is predicted to fold into a highly ordered secondary structure that has been experimentally modelled by computational, phylogenetic, biochemical and mutational probing studies (Damgaard et al., 2004; Kasprzak et al., 2005). Although minor variations exist, the consensus structure involves seven structural stem-loop motifs that represent independent functional elements (Fig. 1): the trans-activation region (TAR), the polyadenylation signal [Poly(A)], the primer binding site (PBS), the dimerisation initiation site (DIS or SL1), the major splice donor site (SD or SL2), the genomic packing signal (Psi, ψ or SL3) and a stem-loop containing the AUG initiation

codon of the Gag open reading frame (AUG or SL4) (Berkhout, 1996). Mutational analysis indicates that the DIS domain is the most important element involved in *in vitro* dimerisation (Laughrea and Jette, 1994; Muriaux et al., 1995; Paillart et al., 1994; Skripkin et al., 1994). Full-length leader RNA can adopt two alternative forms *in vitro*: the thermodynamically favoured leader RNA structure conformation, known as the long distance interaction (LDI) since it involves long distance base pairing between the Poly(A) and DIS (Huthoff and Berkhout, 2001); and the branched multiple hairpins (BMH) conformation. The folding of the BMH exposes the DIS-containing hairpin structure, which has a 6-mer palindromic sequence closing loop (GCGCGC) important in RNA dimerisation. It has been described that only the BMH conformer can dimerise via an intermolecular interaction between the palindromes of two DIS elements (Clever et al., 1996; Haddrick et al., 1996; Laughrea and Jette, 1994; Muriaux et al., 1995; Paillart et al., 1994; Skripkin et al., 1994). This initial structure is termed the kissing loop dimer complex, which subsequently progresses to a more stable extended duplex involving other nucleotides (Laughrea and Jette, 1996a; Laughrea and Jette, 1996b; Muriaux et al., 1996). Recent studies indicate that gRNA dimerisation can be achieved without a functional DIS (Clever and Parslow, 1997; Laughrea et al., 1997; Shen et al., 2000; Shen et al., 2001). This suggests that one or more DIS-independent dimerisation sites exist in HIV-1 gRNA, though their precise molecular location remains unclear. Moreover, the originally identified DLS-encompassing sequence, which included bases 1-311 of the HIV-1 5'UTR, has undergone some refinement. Sakuragi et al. traced the sequence requirements of the DLS to a non-contiguous 144 nt region, consisting of sequences from the junction between the Poly(A) and PBS elements to the end of the AUG-containing stem-loop (more specifically, nucleotide sequences 105-130, 217-281 and

301-352 of the HBX2 strain of HIV-1) (Sakuragi et al., 2007). The roles of these regions in RNA-RNA interactions are still to be properly defined.

Synthetic oligodeoxynucleotides (ODNs) complementary to HIV-1 RNA, and their derivatives, have great potential as tools for investigating the molecular biology of functional RNA elements. In their simplest form, these ODNs are introduced into the cell to block gene expression by interfering with translation of mRNA or by promoting the degradation of the target RNA via an RNase H-dependent pathway. Targeting with antisense ODNs can also provide information on the structure of a target RNA and can be used to block the access of other molecules to specific nucleic acid sequences. Traditionally, researchers attempting to inhibit gene expression with antisense ODNs avoid targeting regions with a stable secondary structure. However, since stable structural RNA domains coincide with important functional elements, they represent potential targets for efficient inhibition. The binding of oligonucleotides to regions in the RNA that are predominantly double-stranded has previously been reported to be associated with a strong antisense response *in vivo* (Laptev et al., 1994). The present study examines the potential of a set of unmodified antisense ODNs directed against the different stemp-loop structural elements of functional importance within the 5'UTR of HIV-1 gRNA, in the analysis of RNA dimerisation *in vitro*. It also examines the capacity of these ODNs to inhibit HIV-1 proliferation and gene expression in cell cultures.

2. Materials and Methods

2.1. Antisense and control oligonucleotides

ODNs were synthesized using an automated Applied Biosystems 3400 DNA synthesizer (Applied Biosystems, Foster City, CA, USA) using standard phosphoramidite chemistry. All ODNs were designed as 30 nt-long molecules, except for the 25 nt-long AUG-as complementary to a specific target site within the HIV-1 5'UTR genomic RNA. All were named according to their target site (Table 1). Two control, non-specific oligonucleotides were designed: pLCX-30, which is complementary to no sequence motif of the HIV-1 genome, and a 30 nt-long random sequence (theoretically containing 7.2×10^{16} sequences).

2.2. DNA templates and RNA synthesis

The DNA template for the synthesis of the HIV-1 5'UTR genomic RNA fragment was obtained by PCR amplification of the pUC18-based pNL4-3 plasmid (Adachi et al., 1986). A T7 RNA-polymerase promoter sequence was incorporated by the sense PCR primer 5'-T7pNL4-3: 5'-**TAATACGACTCACTATAGGG**TCTCT CTGGTTAG-3' (the T7 promoter is indicated in bold). The 3'pNL4-3-gag GCTTAATACCGACGCTCTC was used as a reverse PCR primer. The HIV-1_{NL4-3} 5'UTR RNA fragment containing nucleotides 1-357 was obtained by *in vitro* transcription of the gel-purified PCR product, and purified as previously described (Barroso-delJesus et al., 1999). RNA was renatured by heating to 85°C followed by slow cooling to room temperature prior to use.

2.3. *In vitro* RNase H cleavage assay

Before digestion with *Escherichia coli* RNase H, 0.5 nM of 5' end ^{32}P-labelled RNA transcript was renatured in 10X RNase H buffer (200 mM Tris-HCl pH 7.8, 400 mM KCl, 80 mM $MgCl_2$, 10 mM DTT) by heating at 65°C for 3 min followed by slow

cooling to room temperature. The RNA transcript was incubated separately with each oligonucleotide (1 μM) for 30 min at 37ºC. Subsequently, 5 U of RNase H (Ambion, Austin, TX) was added to the mixtures and incubated at 37°C for 20 min. The reactions were quenched with equal volumes of 2X formamide gel loading buffer and loaded onto a 7 M urea 6% polyacrylamide denaturing gel in 1X TBE buffer. After electrophoretic resolution of the digestion products at 20 mA for approximately 90 min, the gel was vacuum dried and analysed using a Typhoon 9400 scanner (GE Healthcare).

2.4. *In vitro* dimerisation assay

Four picomoles of unlabelled HIV-1_{NL4-3} 5'UTR transcript were added to 8 μl of Milli-Q (Millipore, Rockland, MA) water containing 0.05 pmol of radiolabelled HIV_{NL4-3}-5'UTR and 50 pmol of individual unlabelled antisense oligonucleotides or combinations of antisense oligonucleotides (50 pmol of each ODN included). Samples were denatured at 95ºC (2 min) and snap-cooled on ice. Dimerisation reactions were performed as described by (Sánchez-Luque et al., 2010). Briefly, the dimerisation reaction was initiated by adding 2 μl of 5X dimer buffer (1X: 50 mM sodium cacodylate, pH 7.5, 300 mM KCl and 5 mM $MgCl_2$) at 37ºC for 45 min and then stopped by the addition of 2X gel loading buffer (Tris-acetate 20 mM, Mg acetate 10 mM, NaCl 0.1 M, glycerol 30% v/v, xylene cyanol 0.4% p/v, bromophenol blue 0.4% p/v, tRNA 4% p/v). In parallel, RNA 1-357 was incubated in monomerisation buffer (50 mM sodium cacodylate, pH 7.5, 40 mM KCl and 0.1 mM $MgCl_2$). Samples were analysed on 1% agarose gels in 1X TBM buffer (0.5X Tris-borate, 0.1 mM $MgCl_2$). Electrophoresis (100 V) was performed in the same buffer at 4ºC for 2.5 h. Gels were fixed with 10% trichloroacetic acid for 10 min, dried for 1 h under vacuum at room

temperature, and exposed to phosphorimager screens from 4 h to 'overnight'. The dimerisation efficiency was calculated as [dimmer x 100 / (dimmer + monomer)]. Data are expressed at the mean ± standard deviation of three independent experiments.

2.5. Cell culture and transfection

The human embryonic kidney (HEK) cell-line 293T was maintained in Dulbecco's modified Eagle's medium (DEMN) supplemented with 10% foetal bovine serum (FBS; Gibco Invitrogen, San Diego, CA, USA), 100 µg/ml streptomycin (Sigma Chemical Co. St Louis, MO, USA), 4 mM L-glutamine (Sigma) and 1 mM sodium pyruvate (Sigma). Human T lymphocyte Jurkat cells were maintained in RPMI-1640 supplemented with 10% FBS (Gibco), 4 mM L-glutamine (Sigma) and 100 µg/ml Streptomycin (Sigma). All cells were incubated at 37°C under humidified air containing 5% CO_2.

For the transfection of the HEK 293T cells, 1 X 10^5 cells were seeded in 1 ml of DMEM in 24-well culture plates. For the transfection of the Jurkat cells, 5 x 10^5 cells were seeded in 1 ml of RMPI. Both cell lines were co-transfected with 100 pmol (0.2 µM) of the ODNs and 100 ng of pNL4-3 plasmid complexed with 1 µl Fugene HD (Roche Diagnostics, Mannheim, Germany). At 6 h post-transfection, the HEK 293T cells were provided with fresh growth medium (to remove the transfection mixture) and further incubated at 37°C for 48 h. For the Jurkat cells, the transfection mixture was replaced by fresh growth medium after 4 h. Cells incubated with Fugene HD or medium alone were used as controls. The expression and replication of the HIV-1 proviral clones were then monitored by determining viral p24 antigen in culture supernatants using an enzyme immunoassay (EIA, Bio-Rad Laboratories, Redmond, WA) and employing a Molecular Devices microplate reader. The results were

expressed as the mean ± standard deviation of at least three independent determinations.

2.6. Quantitative real-time RT-PCR assays

Quantitative real time RT-PCR analysis was performed 48 h after co-transfection. Total RNA was extracted with Trizol reagent (Invitrogen, San Diego, CA) according to the manufacturer's protocol. To remove potentially contaminating genomic DNA, all RNA samples were digested with RNase-free RQ1 DNase (Promega, Madison, WI, USA) at 37°C for 30 min followed by phenol-chloroform extraction. Total RNA (1 µg) was reverse transcribed using the High-Capacity cDNA Reverse Transcription Kit (Applied Biosystems) and random hexamers, according to the manufacturer's instructions. The cDNA was used as a template for quantitative qRT-PCR analysis using iTaq Fast SYBR Green Supermix with ROX (Bio-Rad Laboratories, Hercules, CA, USA), following the manufacturer's recommended conditions. Gene expression was normalized to the GAPDH expression levels for data analysis of each sample. The calibrator sample in real-time PCR was the cDNA from HEK 293T cells co-transfected with pLCX-30. Data was analyzed using the comparative cycle threshold (Ct) method, as described (Livak and Schmittgen, 2001).

3. Results

3.1. Accessibility of structural HIV-1 5'UTR functional domains to specific antisense ODNs

Target accessibility is a critical limitation of antisense applications. A set of antisense ODNs targeting the different structural RNA elements within the 5'UTR of HIV-1 RNA

was designed (Table 1; Fig. 1). Access to the targeted genomic RNA domains by the ODNs was tested by RNase H digestion. For this, a 5' end ^{32}P-labelled HIV-1-RNA fragment containing the first 357 nucleotides of HIV-1 gRNA was *in vitro* synthesized and subjected to RNase H digestion in the absence or presence of a molar excess of unlabelled antisense ODNs (Fig. 2). Complete cleavage of the 5'UTR of HIV-1 gRNA was observed in the presence of the oligonucleotides TAR-as, PBS1-as, PBS2-as, PSB3-as, PSB4-as, SD-as, Psi-as and AUG-as, while cleavage efficiency was reduced to 71.4 % and 86.8 % in the presence of Poly(A)-as or DIS-as. These results indicate that the different targeted sequences within the HIV-1 5'UTR structural elements are accessible to their specific ODNs. No cleavage products were detected in the presence of the negative control ODNs pLCX-30 and Random-30.

3.2. Effect of the 5'UTR-antisense ODNs on the *in vitro* dimerisation of HIV-1 RNA

In vitro RNA dimerisation assays were performed in the presence of the specific antisense ODNs targeting each of the functional elements within the 5'UTR, in order to analyse their putative role in this essential viral process. Briefly, 50 pmol of each antisense ODN was independently incubated with 4 pmol of unlabelled HIV-1 RNA 1-357, contaminated with traces of internally ^{32}P-labelled HIV-1 RNA 1-357 (see Materials and methods), which includes the entire 5'UTR and the first 22 nucleotides of *gag* ORF, under the dimerisation conditions described in Materials and Methods (Fig 3). Under these high ionic strength conditions, ≥60% of the 1-357 transcripts entered into a dimer complex (under low ionic strength the monomer status is entirely predominant; no dimers are detected). As expected, nearly complete inhibition of dimer formation was observed in the presence of the DIS antisense ODN (DIS-as),

confirming the DIS element to be the major dimerisation site and corroborating previous observations suggesting dimerisation to be essentially governed by the DIS element taking part in a reversible apical loop-apical loop interaction (Paillart et al., 1996). Strong dimerisation inhibition was also detected when blocking the SD domain with the corresponding antisense ODN (only 24% dimerisation was seen in the presence of SD-as). RNA dimerisation inhibition was also observed with ODNs complementary to the Psi and AUG regions (Fig. 3, Lanes 13 and 14). These results indicate the potential involvement of the SD, Psi and AUG elements in RNA dimerisation. Surprisingly, a larger RNA dimerisation yield (93%) was obtained in the presence of the anti-TAR ODN (TAR-as). This suggests that the TAR element has a negative effect on RNA dimerisation. Similarly, an increase in the dimer yield was observed in the presence of Poly(A)-as, PBS1-as and PBS4-as. No effect was observed in the presence of PBS2-as or PBS3-as (Fig. 3, Lanes 8 and 9), nor in the presence of the control ODNs pLCX-30-as and Random-30-as.

3.3. Interference of the RNA dimerisation by targeting the AUG-containing structural element

A number of authors have indicated that dimerisation can take place in the absence of a functional DIS element. This suggests that other elements act as secondary dimerisation initiation sites (Berkhout, 1996; Haddrick et al., 1996; Sakuragi and Panganiban, 1997; Shen et al., 2000) but whose contribution goes unnoticed in the presence of a functional DIS element. The role in dimerisation of the different structural elements within the 5'UTR was therefore examined in a DIS-depleted functional background. For this, *in vitro* dimerisation was assayed in the presence of a combination of specific ODNs and DIS-as (to obtain the required background) (Fig.

4). No inhibitory effect beyond that associated with DIS-as was observed with the addition of the ODNs SD-as or Psi-as (Fig. 4; compare Lanes 5 and 6 to Lane 4), suggesting that SD and Psi played no direct or DIS-independent role in RNA dimerisation. Interestingly, the subsequent addition of AUG-as abolished the formation of RNA dimers (Fig. 4, Lane 7). This, together with the partial inhibitory effect observed when blocking only the AUG region (Fig. 3, Lane 14), suggests that the AUG region may play a direct role in RNA dimerisation, though we cannot rule out the possibility of an indirect effect on dimerisation due to the induction of structural modifications in the HIV RNA. Finally, the addition of TAR-as (Fig. 4, Lane 8) partially restored the dimerisation capability of the gRNA, which is in good agreement with results shown in Figure 3.

3.4. Involvement of the PBS element in RNA dimerisation

An analysis of the potential role in RNA dimerisation of the structural domain containing the PBS element was undertaken in a DIS-blocked background (Fig. 5). The addition of PBS1-as or PBS4-as resulted in no significant effect (compare Lanes 3 and 6 with Lane 2). However, a clear promotion of RNA dimerisation was observed in the presence of PBS2-as or PBS3-as or both. These results indicate that their nt 107-136 and 142-171 target regions might negatively affect dimerisation. Interestingly, when PBS2-as and/or PBS3-as were combined with PBS1-as, but not with PBS4-as, the efficiency of dimerisation was inhibited. This suggests that the target sequence of the PBS1-as (nt 210-239) in the structural motif-containing the PBS element may play a direct role in promoting HIV-1 gRNA dimerisation.

3.5. Inhibition of HIV-1 production and gene expression by antisense oligonucleotides

All the targeted HIV-1 structural elements play essential roles in the viral cycle. Since the antisense ODNs bound efficiently to the different functional 5'UTR structural elements, their effect on viral particles production and HIV-1 gene expression in cell culture was also tested. For this, HEK 293T and Jurkat cells were co-transfected with the pNL4-3 plasmid and a set of specific ODNs. Transfection with pro-viral DNA mimics the post-integration stage of the viral cycle. The effect of the antisense ODNs measured as viral p24 antigen levels in the supernatant, in both cell lines was quantified at 48 h post-transfection, at which viral particles in the supernatant should correspond to first generation virions. A reduction in viral production was observed with Poly(A)-as, pBS1-as pBS2-as, pBS3-as, SD-as and Psi-as (Fig. 6),whereas no inhibitory effect was seen for TAR-as, PBS4-as or DIS-as. These results suggest that Poly(A)-as, pBS1-as pBS2-as, pBS3-as, SD-as and Psi-as are functional in cells of lymphoid origin, and highlight the potential of the motifs they seek out as antiviral targets in human T cell cultures.

Antisense activity might be achieved through RNase H-mediated degradation of the target RNA. To confirm that the ODNs reduced the steady-state levels of HIV-1 RNA in co-transfected HEK 293T cells, HIV-1-5'UTR RNA was quantified by real time RT-PCR at 48 h post-transfection. The results in Figure 7 show a significant reduction in viral RNA after transient transfection with Poly(A)-as, pBS1-as pBS2-as, pBS3-as, SD-as, Psi-as and AUG-as; this correlates perfectly with the reduction seen in viral p24 antigen levels (Fig. 6).

4. Discussion

A major concern in the design of efficient antisense ODNs against highly structured viral RNA genomes is the accessibility of the target sequences. A correlation between *in vitro* accessibility and the intracellular activity of antisense ODNs has been reported for several target RNAs (Ho et al., 1998; Ho et al., 1996; Matveeva et al., 1997; Southern et al., 1997). Since the HIV-1 5'UTR is folded into a complex secondary and tertiary structure, it might be thought that many potential target sites become inaccessible. However, the present results indicate that the different structural elements of the 5'UTR remain accessible to antisense ODNs (Fig. 2). The partial discrepancies with the results of other authors (Ooms et al., 2004) in terms of 5'UTR accessibility may be due to differences in the experimental conditions, the length of the oligonucleotides used, or differences in the target sequences.

Deletions that affect the TAR element are thought to result in increased *in vitro* HIV-1-RNA dimerisation (Vrolijk et al., 2008). This would agree with the effects observed in the present work when TAR-as was introduced into the system (Fig. 3, Lane 5; Fig. 4, Lane 8). Although the TAR element itself is not directly involved in the switch from LDI to BMH conformers -since it is conserved in both conformations- the destabilisation of TAR may affect LDI-BMH equilibrium and thus indirectly influence other functional RNA elements. In contrast to that seen in the present work, evidence exists that the TAR element makes a positive contribution to RNA dimerisation *in vitro* (Andersen et al., 2004). However, the latter authors performed their dimerisation assays in the presence of the nucleocapsid protein, which may explain the lack of agreement with the present data. The validation of these *in vitro* interaction studies in a cellular system that permits viral replication is essential since different long-range

RNA-RNA interactions, among other factors, might influence the ability of HIV-1 RNA to dimerise.

DIS-as essentially blocked dimerisation, probably sequestering the palindromic sequences in the DIS loop, and interfering in the kissing-loop interaction. The *in vitro* dimerisation inhibition exerted by SD-as might be a consequence of the close proximity of its 3' end binding site to the highly conserved AGG loop at the base of the DIS element stem (position 271-273), which has been implicated in dimerisation (Clever and Parslow, 1997; Greatorex et al., 2002; Takahashi et al., 2000). SD-as may have also an indirect effect on dimerisation via its altering the structure of the DIS element; this may affect the distal-loop sequence involved in the kissing-loop interaction. Blocking of the SD structural domain partially inhibited RNA dimerisation (Fig. 3), but no additional inhibitory effect was observed when it was combined with DIS-as (Fig. 4). Similar behaviour was recorded with respect to the modest inhibition achieved with Psi-as. These results suggest that SD and Psi play no DIS-independent role in RNA dimerisation. According with a previous work describing that destabilization of the LDI conformer by targeting the 5' UTR with oligonucleotides induced the switch to the BMH dimerisation competent conformer (Berkhout et al., 2002), the ODN effects described here can be attributed to structure alterations challenging the DIS functionality.

Interestingly, the remaining RNA dimerisation activity observed in the presence of DIS-as, SD-as and Psi-as was abolished with the addition of AUG-as (Fig. 4). Since this effect was observed in a DIS-blocked background our data suggest that the sequence surrounding the AUG initiation codon might provide a dimerisation site. Nevertheless we cannot discard an indirect effect of the AUG-as by affecting the structure of the 5'UTR influencing the exposure of a hypothetically remaining

functional DIS element responsible of the observed 10% of RNA dimmers in the presence of the DIS-as. A long-distance base pairing between the linker sequences of poly(A) and the PBS elements plus the nucleotides surrounding the AUG Gag initiation codon has been described (Abbink and Berkhout, 2003). The resulting interaction yields the so called U5-AUG duplex. This may explain the present results that suggest the AUG-containing domain might play a direct role in RNA dimerisation. Such a role is supported by the observation that the AUG effect is summatory to that associated with DIS rather than synergistic. DIS-as reduces dimerisation from 60% to 10%, AUG-as from 60% to 50% and both from 60% to 0%, suggesting that the effects of these two regions are independent of one another.

Evidence that the extended PBS-containing stem-loop motif contributes to gRNA dimerisation was first provided by the effect of deleting nt 200-226 or 236-242 in virions produced by Cos-7 cells (Shen et al., 2000). The present results show that while antisense ODNs targeting the 5' strand of the PBS-containing the stem-loop motif have little or no impact on gRNA dimerisation (PBS2-as and PBS3-as), blocking the 3' end nt positions 178-207 and 210-239 segments with PBS4-as and PBS1-as respectively promoted dimerisation in a functional DIS background (Fig. 3). However, in a non-functional DIS background, clear promotion of dimerisation was observed when the region comprised between nt 210 and 239 was accessible (Fig. 5). The negative effect of other regions of the PBS-containing structural motif may be due to the sequestering of the nt 210-239 sequences. Thus it seems necessary to block its complementary sequence with PBS2-as for the promotion of dimerisation by the sequences at the 3' end of the PBS-containing element to occur. It is noteworthy that this region contains an imperfect palindromic sequence (GAGAUCUCUC), and that this might be involved in this process. Further (Sakuragi et al., 2012) have recently

found highly conserved complementary sequences located upstream of the DIS stem (GACGC) and at the 3' end of the DLS (GCGUC). Their data strongly suggest that both sequences interact and the duplex formation (GACGC-GCGUC) occurs within the virus playing an important role for DLS function. Interestingly, in our dimerisation assays the sequence GACGC is blocked by the PSB1-as. In a functional DIS background the opposite effect to that observed with PBS1-as and PBS4-as may be due to the stabilisation of the functional DIS structural motif.

In addition to their effect on dimerisation, the assayed antisense ODNs may interfere with other essential steps in the viral cycle. This would explain the significant antiviral activity of Poly(A)-as, PBS1-as, PBS2-as, PBS3-as, SD-as, Psi-as and AUG-as observed in cell culture. Antisense ODNs targeting the PBS1, PBS2 or PBS3 sequences may interfere with tRNA binding to the PBS motif and the subsequent initiation of reverse transcription. SD-as covers the major splice donor site and may therefore interfere with splice site recognition, but also with RNA packaging since the SD region contributes to this process (Amarasinghe et al., 2000; Amarasinghe et al., 2001). Psi-as may interfere with genomic RNA encapsidation. Finally AUG-as may block the HIV translation initiation. Nevertheless we cannot discard an effect of the ODNs on the viral infectious DNA.

5. Conclusions

The present results show that antisense oligonucleotides are excellent tools for deciphering the functional implications of structural RNA domains, and provide evidence that may suggests a direct role of the AUG-containing RNA element and the 3' end sequence of the PBS-containing structural domain in the dimerisation of

genomic HIV-1 RNA. In contrast, the apical portion of the TAR stem-loop element seems to play a negative role in RNA dimerisation. ODNs are also shown to be excellent tools for exploring the potential of conserved structural RNA elements as antiviral targets.

Acknowledgements

The authors thank Drs. Jordi Gómez and Cristina Romero-López for critically reading the manuscript and offering valuable suggestions and Dr. Francisco Muñoz for helping in the preparation of figure 1. We are also indebted to Vicente Augustin Vacas for excellent technical assistance. This work was supported by grants BFU2006-02508 and BFU2009-08137 from the Spanish *Ministerio de Ciencia e Innovación*, FIPSE 36472/05 to A. B-H. J.A.R-D. was funded by grant 36472/05 from the FIPSE. Work at our laboratory is partially supported by FEDER funds from the EU.

References

Abbink, T.E. and Berkhout, B. (2003) A novel long distance base-pairing interaction in human immunodeficiency virus type 1 RNA occludes the Gag start codon. J Biol Chem 278(13), 11601-11.

Adachi, A., Gendelman, H.E., Koenig, S., Folks, T., Willey, R., Rabson, A. and Martin, M.A. (1986) Production of acquired immunodeficiency syndrome-associated retrovirus in human and nonhuman cells transfected with an infectious molecular clone. J Virol 59(2), 284-91.

Amarasinghe, G.K., De Guzman, R.N., Turner, R.B., Chancellor, K.J., Wu, Z.R. and Summers, M.F. (2000) NMR structure of the HIV-1 nucleocapsid protein bound to stem-loop SL2 of the psi-RNA packaging signal. Implications for genome recognition. J Mol Biol 301(2), 491-511.

Amarasinghe, G.K., Zhou, J., Miskimon, M., Chancellor, K.J., McDonald, J.A., Matthews, A.G., Miller, R.R., Rouse, M.D. and Summers, M.F. (2001) Stem-loop SL4 of the HIV-1 psi RNA packaging signal exhibits weak affinity for the nucleocapsid protein. structural studies and implications for genome recognition. J Mol Biol 314(5), 961-70.

Andersen, E.S., Contera, S.A., Knudsen, B., Damgaard, C.K., Besenbacher, F. and Kjems, J. (2004) Role of the trans-activation response element in dimerization of HIV-1 RNA. J Biol Chem 279(21), 22243-9.

Barroso-delJesus, A., Tabler, M. and Berzal-Herranz, A. (1999) Comparative kinetic analysis of structural variants of the hairpin ribozyme reveals further potential to optimize its catalytic performance. Antisense Nucleic Acid Drug Dev 9(5), 433-40.

Bender, W. and Davidson, N. (1976) Mapping of poly(A) sequences in the electron microscope reveals unusual structure of type C oncornavirus RNA molecules. Cell 7(4), 595-607.

Berkhout, B. (1996) Structure and function of the human immunodeficiency virus leader RNA. Prog Nucleic Acid Res Mol Biol 54, 1-34.

Berkhout, B., Ooms, M., Beerens, N., Huthoff, H., Southern, E. and Verhoef, K. (2002) In vitro evidence that the untranslated leader of the HIV-1 genome is an RNA checkpoint that regulates multiple functions through conformational changes. J Biol Chem 277(22), 19967-75.

Clever, J.L. and Parslow, T.G. (1997) Mutant human immunodeficiency virus type 1 genomes with defects in RNA dimerization or encapsidation. J Virol 71(5), 3407-14.

Clever, J.L., Wong, M.L. and Parslow, T.G. (1996) Requirements for kissing-loop-mediated dimerization of human immunodeficiency virus RNA. J Virol 70(9), 5902-8.

Damgaard, C.K., Andersen, E.S., Knudsen, B., Gorodkin, J. and Kjems, J. (2004) RNA interactions in the 5' region of the HIV-1 genome. J Mol Biol 336(2), 369-79.

Darlix, J.L., Gabus, C., Nugeyre, M.T., Clavel, F. and Barre-Sinoussi, F. (1990) Cis elements and trans-acting factors involved in the RNA dimerization of the human immunodeficiency virus HIV-1. J Mol Biol 216(3), 689-99.

Fu, W. and Rein, A. (1993) Maturation of dimeric viral RNA of Moloney murine leukemia virus. J Virol 67(9), 5443-9.

Gotte, M., Li, X. and Wainberg, M.A. (1999) HIV-1 reverse transcription: a brief overview focused on structure-function relationships among molecules involved in initiation of the reaction. Arch Biochem Biophys 365(2), 199-210.

Greatorex, J., Gallego, J., Varani, G. and Lever, A. (2002) Structure and stability of wild-type and mutant RNA internal loops from the SL-1 domain of the HIV-1 packaging signal. J Mol Biol 322(3), 543-57.

Haddrick, M., Lear, A.L., Cann, A.J. and Heaphy, S. (1996) Evidence that a kissing loop structure facilitates genomic RNA dimerisation in HIV-1. J Mol Biol 259(1), 58-68.

Ho, S.P., Bao, Y., Lesher, T., Malhotra, R., Ma, L.Y., Fluharty, S.J. and Sakai, R.R. (1998) Mapping of RNA accessible sites for antisense experiments with oligonucleotide libraries. Nat Biotechnol 16(1), 59-63.

Ho, S.P., Britton, D.H., Stone, B.A., Behrens, D.L., Leffet, L.M., Hobbs, F.W., Miller, J.A. and Trainor, G.L. (1996) Potent antisense oligonucleotides to the human multidrug resistance-1 mRNA are rationally selected by mapping RNA-accessible sites with oligonucleotide libraries. Nucleic Acids Res 24(10), 1901-7.

Hoglund, S., Ohagen, A., Goncalves, J., Panganiban, A.T. and Gabuzda, D. (1997) Ultrastructure of HIV-1 genomic RNA. Virology 233(2), 271-9.

Huthoff, H. and Berkhout, B. (2001) Two alternating structures of the HIV-1 leader RNA. RNA 7(1), 143-57.
Kasprzak, W., Bindewald, E. and Shapiro, B.A. (2005) Structural polymorphism of the HIV-1 leader region explored by computational methods. Nucleic Acids Res 33(22), 7151-63.
Laptev, A.V., Lu, Z., Colige, A. and Prockop, D.J. (1994) Specific inhibition of expression of a human collagen gene (COL1A1) with modified antisense oligonucleotides. The most effective target sites are clustered in double-stranded regions of the predicted secondary structure for the mRNA. Biochemistry 33(36), 11033-9.
Laughrea, M. and Jette, L. (1994) A 19-nucleotide sequence upstream of the 5' major splice donor is part of the dimerization domain of human immunodeficiency virus 1 genomic RNA. Biochemistry 33(45), 13464-74.
Laughrea, M. and Jette, L. (1996a) HIV-1 genome dimerization: formation kinetics and thermal stability of dimeric HIV-1Lai RNAs are not improved by the 1-232 and 296-790 regions flanking the kissing-loop domain. Biochemistry 35(29), 9366-74.
Laughrea, M. and Jette, L. (1996b) Kissing-loop model of HIV-1 genome dimerization: HIV-1 RNAs can assume alternative dimeric forms, and all sequences upstream or downstream of hairpin 248-271 are dispensable for dimer formation. Biochemistry 35(5), 1589-98.
Laughrea, M., Jette, L., Mak, J., Kleiman, L., Liang, C. and Wainberg, M.A. (1997) Mutations in the kissing-loop hairpin of human immunodeficiency virus type 1 reduce viral infectivity as well as genomic RNA packaging and dimerization. J Virol 71(5), 3397-406.
Livak, K.J. and Schmittgen, T.D. (2001) Analysis of relative gene expression data using real-time quantitative PCR and the 2(-Delta Delta C(T)) Method. Methods 25(4), 402-8.
Marquet, R., Paillart, J.C., Skripkin, E., Ehresmann, C. and Ehresmann, B. (1994) Dimerization of human immunodeficiency virus type 1 RNA involves sequences located upstream of the splice donor site. Nucleic Acids Res 22(2), 145-51.
Matveeva, O., Felden, B., Audlin, S., Gesteland, R.F. and Atkins, J.F. (1997) A rapid in vitro method for obtaining RNA accessibility patterns for complementary DNA probes: correlation with an intracellular pattern and known RNA structures. Nucleic Acids Res 25(24), 5010-6.
Muriaux, D., Fosse, P. and Paoletti, J. (1996) A kissing complex together with a stable dimer is involved in the HIV-1Lai RNA dimerization process in vitro. Biochemistry 35(15), 5075-82.
Muriaux, D., Girard, P.M., Bonnet-Mathoniere, B. and Paoletti, J. (1995) Dimerization of HIV-1Lai RNA at low ionic strength. An autocomplementary sequence in the 5' leader region is evidenced by an antisense oligonucleotide. J Biol Chem 270(14), 8209-16.
Ooms, M., Verhoef, K., Southern, E., Huthoff, H. and Berkhout, B. (2004) Probing alternative foldings of the HIV-1 leader RNA by antisense oligonucleotide scanning arrays. Nucleic Acids Res 32(2), 819-27.
Paillart, J.C., Marquet, R., Skripkin, E., Ehresmann, B. and Ehresmann, C. (1994) Mutational analysis of the bipartite dimer linkage structure of human immunodeficiency virus type 1 genomic RNA. J Biol Chem 269(44), 27486-93.

Paillart, J.C., Shehu-Xhilaga, M., Marquet, R. and Mak, J. (2004) Dimerization of retroviral RNA genomes: an inseparable pair. Nat Rev Microbiol 2(6), 461-72.
Paillart, J.C., Skripkin, E., Ehresmann, B., Ehresmann, C. and Marquet, R. (1996) A loop-loop "kissing" complex is the essential part of the dimer linkage of genomic HIV-1 RNA. Proc Natl Acad Sci U S A 93(11), 5572-7.
Sakuragi, J., Sakuragi, S. and Shioda, T. (2007) Minimal region sufficient for genome dimerization in the human immunodeficiency virus type 1 virion and its potential roles in the early stages of viral replication. J Virol 81(15), 7985-92.
Sakuragi, J.I., Ode, H., Sakuragi, S., Shioda, T. and Sato, H. (2012) A proposal for a new HIV-1 DLS structural model. Nucleic Acids Res. doi:10.1093/nar/gks156.
Sakuragi, J.I. and Panganiban, A.T. (1997) Human immunodeficiency virus type 1 RNA outside the primary encapsidation and dimer linkage region affects RNA dimer stability in vivo. J Virol 71(4), 3250-4.
Sánchez-Luque, F.J., Reyes-Darias, J.A., Puerta-Fernández, E. and Berzal-Herranz, A. (2010) Inhibition of HIV-1 replication and dimerization interference by dual inhibitory RNAs. Molecules 15(7), 4757-72.
Shen, N., Jette, L., Liang, C., Wainberg, M.A. and Laughrea, M. (2000) Impact of human immunodeficiency virus type 1 RNA dimerization on viral infectivity and of stem-loop B on RNA dimerization and reverse transcription and dissociation of dimerization from packaging. J Virol 74(12), 5729-35.
Shen, N., Jette, L., Wainberg, M.A. and Laughrea, M. (2001) Role of stem B, loop B, and nucleotides next to the primer binding site and the kissing-loop domain in human immunodeficiency virus type 1 replication and genomic-RNA dimerization. J Virol 75(21), 10543-9.
Skripkin, E., Paillart, J.C., Marquet, R., Ehresmann, B. and Ehresmann, C. (1994) Identification of the primary site of the human immunodeficiency virus type 1 RNA dimerization in vitro. Proc Natl Acad Sci U S A 91(11), 4945-9.
Southern, E.M., Milner, N. and Mir, K.U. (1997) Discovering antisense reagents by hybridization of RNA to oligonucleotide arrays. Ciba Found Symp 209, 38-44; discussion 44-6.
Takahashi, K., Baba, S., Hayashi, Y., Koyanagi, Y., Yamamoto, N., Takaku, H. and Kawai, G. (2000) NMR analysis of intra- and inter-molecular stems in the dimerization initiation site of the HIV-1 genome. J Biochem 127(4), 681-6.
Vrolijk, M.M., Ooms, M., Harwig, A., Das, A.T. and Berkhout, B. (2008) Destabilization of the TAR hairpin affects the structure and function of the HIV-1 leader RNA. Nucleic Acids Res 36(13), 4352-63.

Figure legends:

Figure 1. Sequence and secondary structure of the 5'UTR of HIV-1. Sequence and secondary structural model of the 5’UTR of the HIV-1 gRNA adapted from Berkhout (Berkhout, 1996). The main stem-loop structural domains associated with

known functions are shown. Antisense ODNs are indicated by a solid line mapping their corresponding complementary target sequences within the HIV-1 5'UTR.

Figure 2. **Accessibility of target structural domains within the HIV-1 5'UTR.** Representative autoradiograph of an electrophoretic gel resolving the RNase H-cleaved RNA fragments of the HIV-1 5'UTR in the presence of different antisense ODNs (indicated at the top of each lane). Lane 13: undigested full length ^{32}P-labelled HIV-1 5'UTR transcript. M: RNA size marker (Century marker, Ambion).

Figure 3. *In vitro* effect of antisense oligonucleotides on the dimerisation of HIV-1 gRNA. Autoradiograph of a representative electrophoretic gel from an RNA dimerisation assay. HIV-1 5'UTR transcript (1-357 nt) was incubated under monomerisation (Lane 1) and dimerisation conditions in the absence (lane 2) and presence of specific antisense ODNs (indicated at the top of the gel). The positions of dimer (D) and monomer (M) RNA species are indicated with arrowheads to the left of the gel. Dimerisation efficiency, indicated below, indicated at the bottom, represents the average of three independent experiments ± SD.

Figure 4. The AUG-containing structural domain promotes HIV-1 RNA dimerisation. Autoradiograph of a representative electrophoretic gel from an RNA dimerisation assay. HIV-1 5'UTR transcript (1-357 nt) was incubated under dimerisation conditions in the presence (+) or absence (–) of different combinations of antisense ODNs (indicated at the bottom of the gel). The positions of monomer (M) and dimer (D) RNA species are indicated with arrowheads at the left. Lane 1, HIV-1 5'UTR transcript incubated under monomeric conditions. Dimerisation efficiency,

indicated at the bottom, represents the average of three independent experiments ± SD.

Figure 5. **The 3' end sequence of the PBS-containing structural domain promotes HIV-1 RNA dimerisation.** Autoradiograph of a representative electrophoretic gel from an RNA dimerisation assay. HIV-1 5'UTR transcript (1-357 nt) was incubated under dimerisation conditions in the presence (+) or absence (-) of different combinations of antisense ODNs (indicated at the bottom of the gel). The positions of monomer (M) and dimer (D) RNA species are indicated with arrowheads at the left. Dimerisation efficiency, indicated at the bottom represents the average of at least three independent experiments ± SD.

Figure 6. Inhibition of HIV-1 replication in human cells. (A) HEK 293T and (B) Jurkat cells were co-transfected with 100 ng of pNL4-3 plasmid and 100 pmol of control or antisense ODNs. Viral production was determined by measuring viral p24 antigen in the supernatant 48 h after co-transfection. The data shown represent the average of at least three independent experiments; standard deviations are indicated by the error bars.

Figure 7. Reduction of HIV-1 RNA levels in human cells by antisense ODNs. HEK 293T cells were co-transfected with 100 ng of pNL4-3 plasmid and 100 pmol of antisense ODNs. After 48 h of co-transfection, total RNA was extracted from the HEK 293T cells and the 5'UTR of the HIV-1 RNA content quantified. RNA amounts are represented as a percentage of the RNA level in the presence of the control pLCX-30 ODN. The results are the mean of three independent experiments.

1

Table 1

ODN	Sequence (5' to 3')	HIV-1_{NL4-3} 5'UTR binding site
pLCX-30 (control)	**GACGTCGAGTGCCCGAAGGATAGCTATCAG**	-
Random-30 (control)	**N_{30}**	-
TAR-1-as	**AGCCAGAGAGCTCCCAGGCTCAGATCTGGT**	**16-45**
Poly(A)-as	**GAGCACTCAAGGCAAGCTTTATTGAGGCTT**	**95-66**
PBS1-as	**TGCGTCGAGAGATCTCCTCTGGCTTTACTT**	**210-239**
PBS2-as	**TAGTTACCAGAGTCACACAACAGACGGGCA**	**107-136**
PBS3-as	**TTT TCCACACTGACTAAAAGGGTCTGAGGG**	**142-171**
PBS4-as	**GCTTTCAAGTCCCTGTTCGGGCGCCACTGC**	**178-207**
DIS-as	**CTCTTGCCGTGCGCGCTTCAGCAAGCCGAG**	**243-252**
SD-as	**TTTGGCGTACTCACCAGTCGCCGCCCCTCG**	**274-303**
Psi-as	**CTC TCCTTCTAGCCTCCGCTAGTCAAAATT**	**304-333**
AUG-as	**CTCTCGCACCCATCTCTCTCCTTCT**	**325-348**

Table 1. Antisense and control ODN sequences used in this study. The nt coordinates of the binding sites are based on Figure 1. N=A, C, G, or T

Figure 1

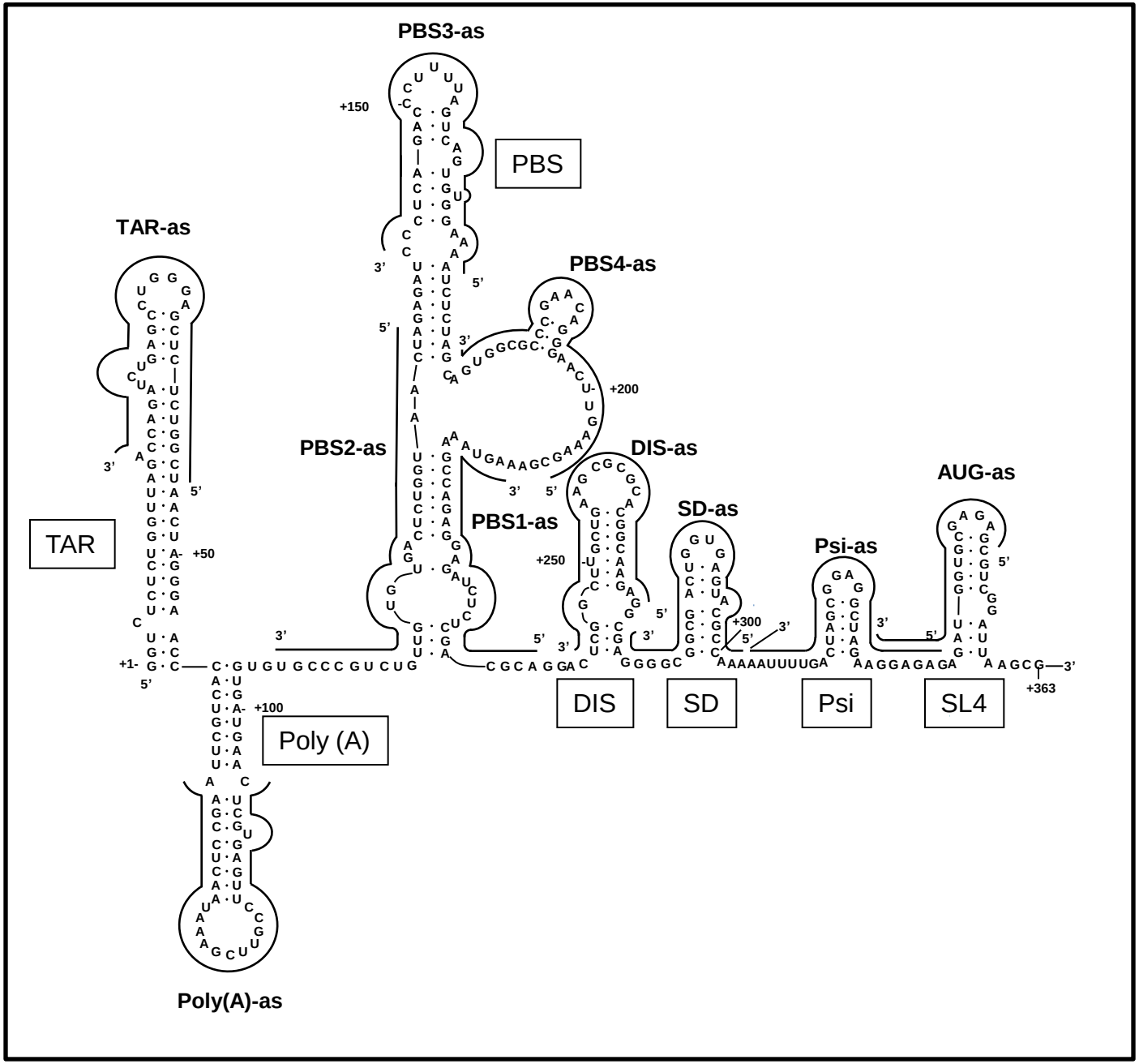
PBS3-as
PBS
TAR-as
PBS4-as
PBS2-as
DIS-as
PBS1-as
AUG-as
SD-as
Psi-as
TAR
DIS
SD
Psi
SL4
Poly (A)
Poly(A)-as
+150
+200
+250
+300
+50
+100
+1-
+363

Figure 2

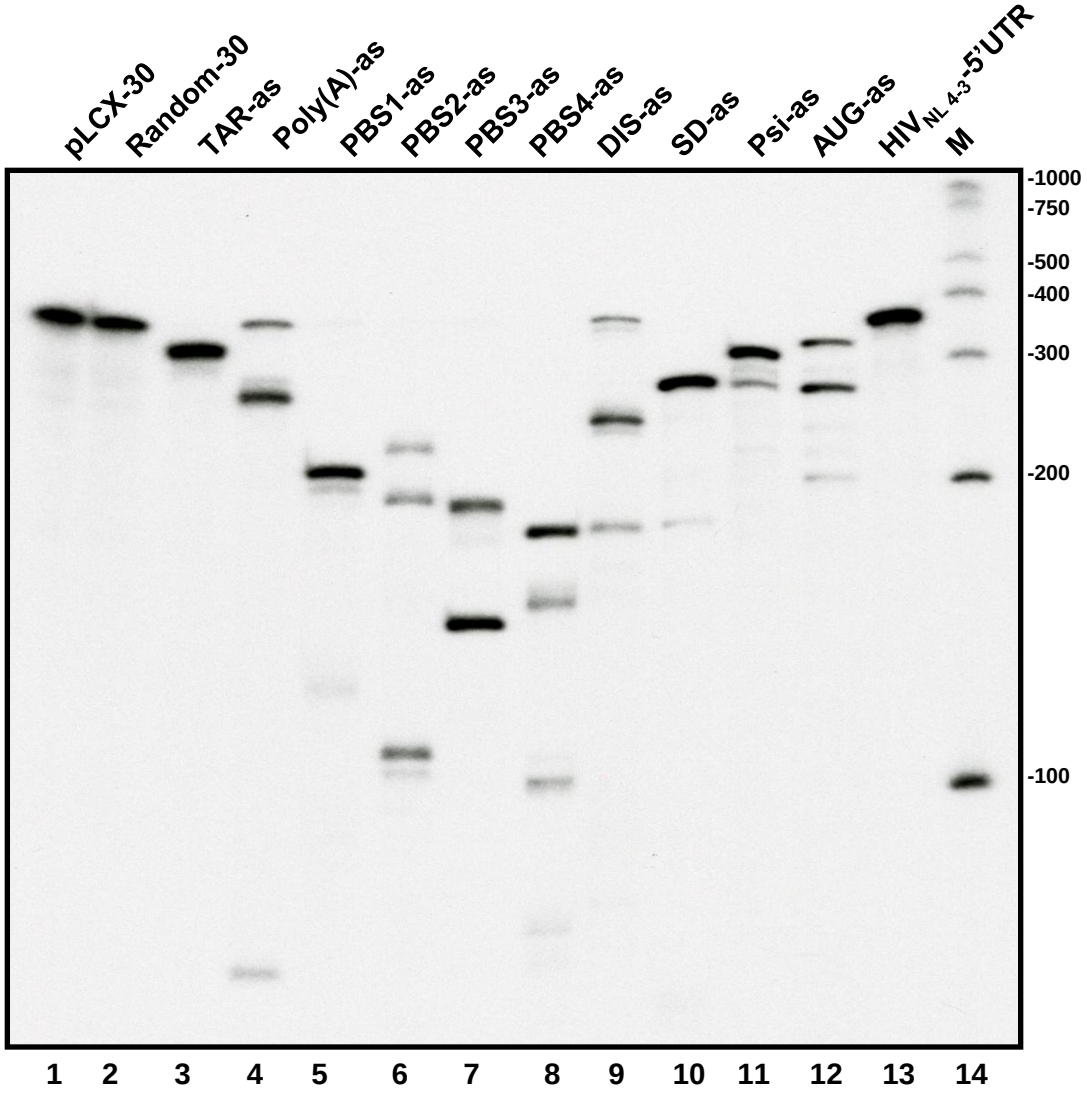
pLCX-30
Random-30
TAR-as
Poly(A)-as
PBS1-as
PBS2-as
PBS3-as
PBS4-as
DIS-as
SD-as
Psi-as
AUG-as
HIV NL 4-3 -5'UTR
M
-1000
-750
-500
-400
-300
-200
-100
1 2 3 4 5 6 7 8 9 10 11 12 13 14

Figure 3

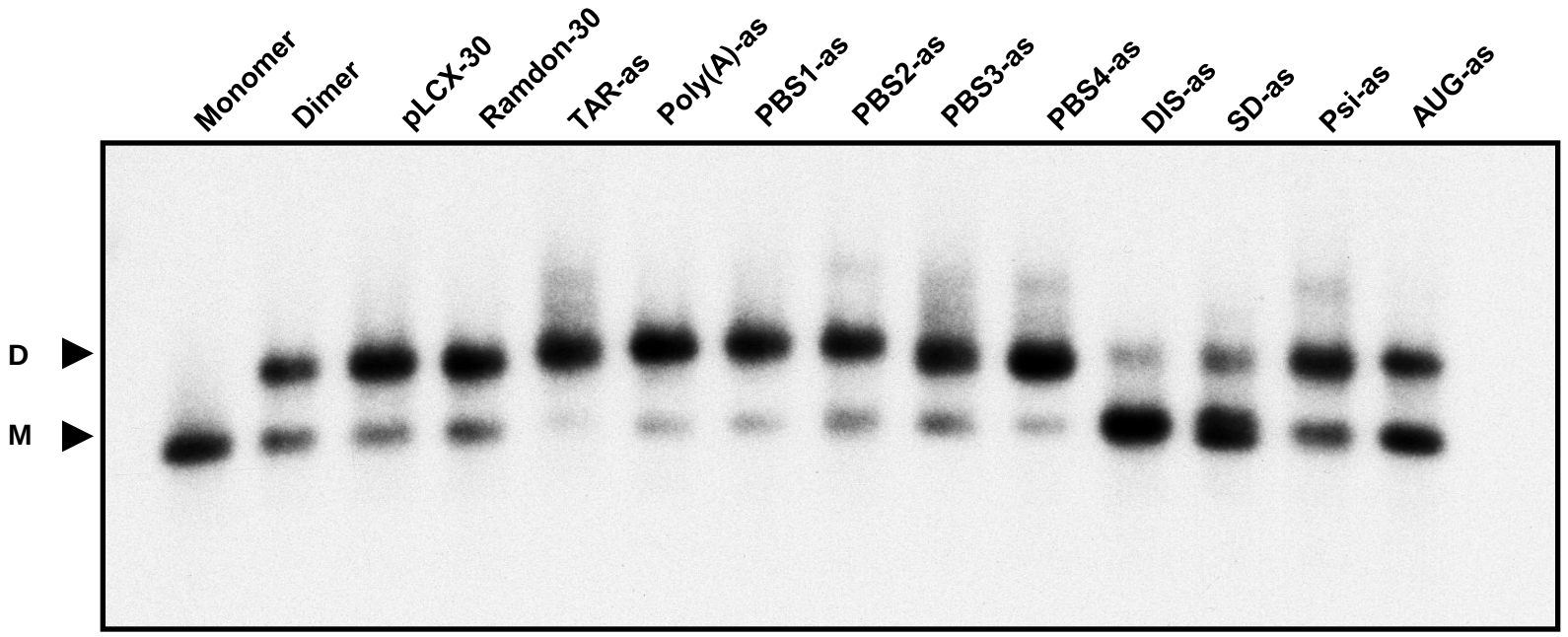

% dimer	-	67.5	0.7	93.2	0.4	78.3	0.3	63.4	0.6	10.9	2.3	53.7	1.6
	60.3	0.4	63.7	1.7	79.7	0.8	66.6	1.1	79.7	0.8	24.4	0.9	49.7	1.1

Figure 4

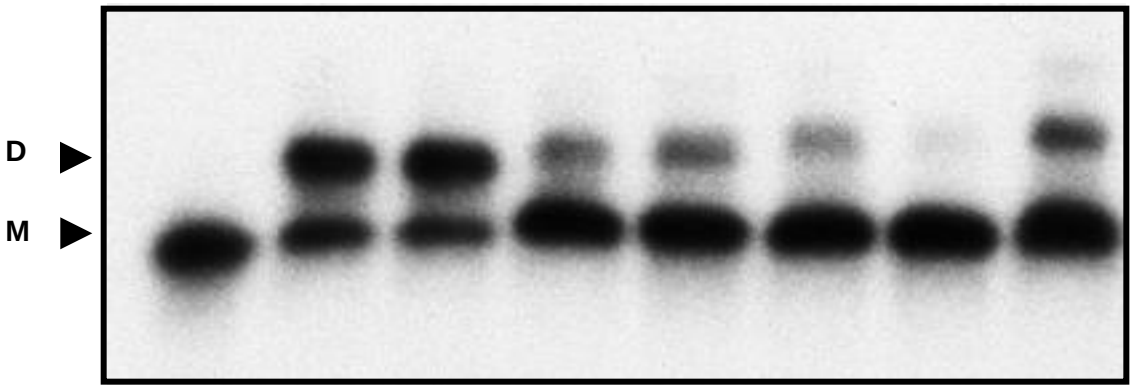

	1	2	3	4	5	6	7	8
pLCX-30	-	-	+	-	-	-	-	-
DIS-as	-	-	-	+	+	+	+	+
SD-as	-	-	-	-	+	+	+	+
Psi-as	-	-	-	-	-	+	+	+
AUG-as	-	-	-	-	-	-	+	+
TAR-as	-	-	-	-	-	-	-	+
% dimer	-	60.5 1,1	63.2 2.3	18.4 1.0	20.9 2.1	14.1 0.7	7.0 0.4	23.9 0.8

Figure 5

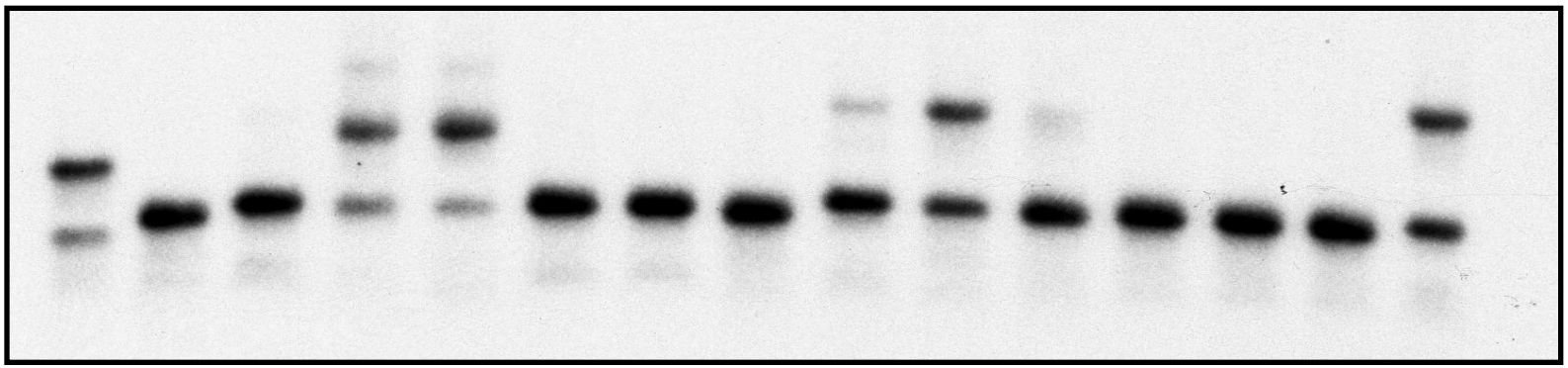

DIS-as	-	+	+	+	+	+	+	+	+	+	+	+	+	+	+
SD-as	-	+	+	+	+	+	+	+	+	+	+	+	+	+	+
Psi-as	-	+	+	+	+	+	+	+	+	+	+	+	+	+	+
AUG-as	-	+	+	+	+	+	+	+	+	+	+	+	+	+	+
PBS1-as	-	-	+	-	-	-	+	+	+	-	-	+	+	+	-
PBS2-as	-	-	-	+	-	-	+	-	-	+	-	+	+	-	+
PBS3-as	-	-	-	-	+	-	-	+	-	+	+	+	-	+	+
PBS4-as	-	-	-	-	-	+	-	-	+	-	+	-	+	+	+

% dimer	60.0	0.5	6.3	0.7	69.9	1.3	5.9	0.0	14.1	0.8	15.5	0.8	4.8	0.2	41.8	2.8
	3.7	0.3	52.3	1.8	5.3	0.1	3.2	0.3	49.7	1.3	3.6	0.4	6.0	0.7		

Figure 6

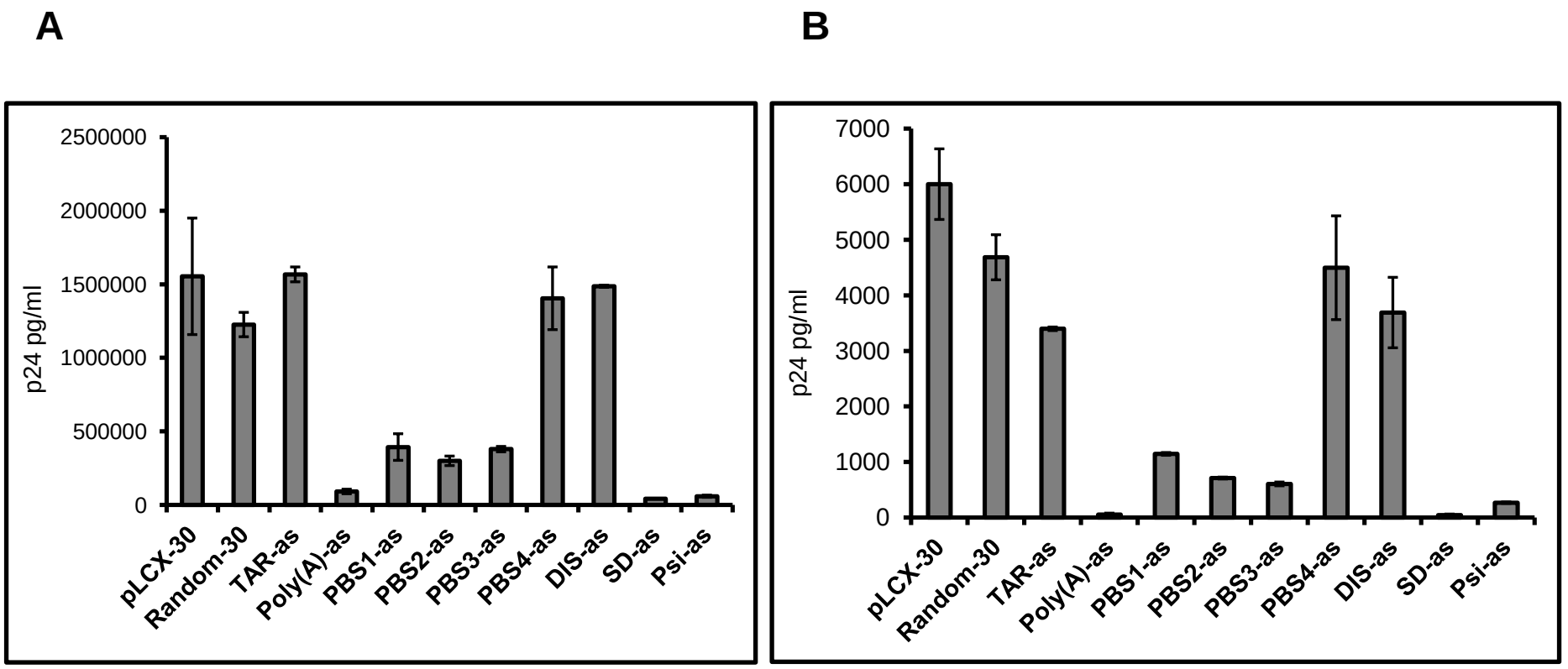
A
B
p24 pg/ml
2500000
2000000
1500000
1000000
500000
0
7000
6000
5000
4000
3000
2000
1000
pLCX-30
Random-30
TAR-as
Poly(A)-as
PBS1-as
PBS2-as
PBS3-as
PBS4-as
DIS-as
SD-as
Psi-as

Figure 7

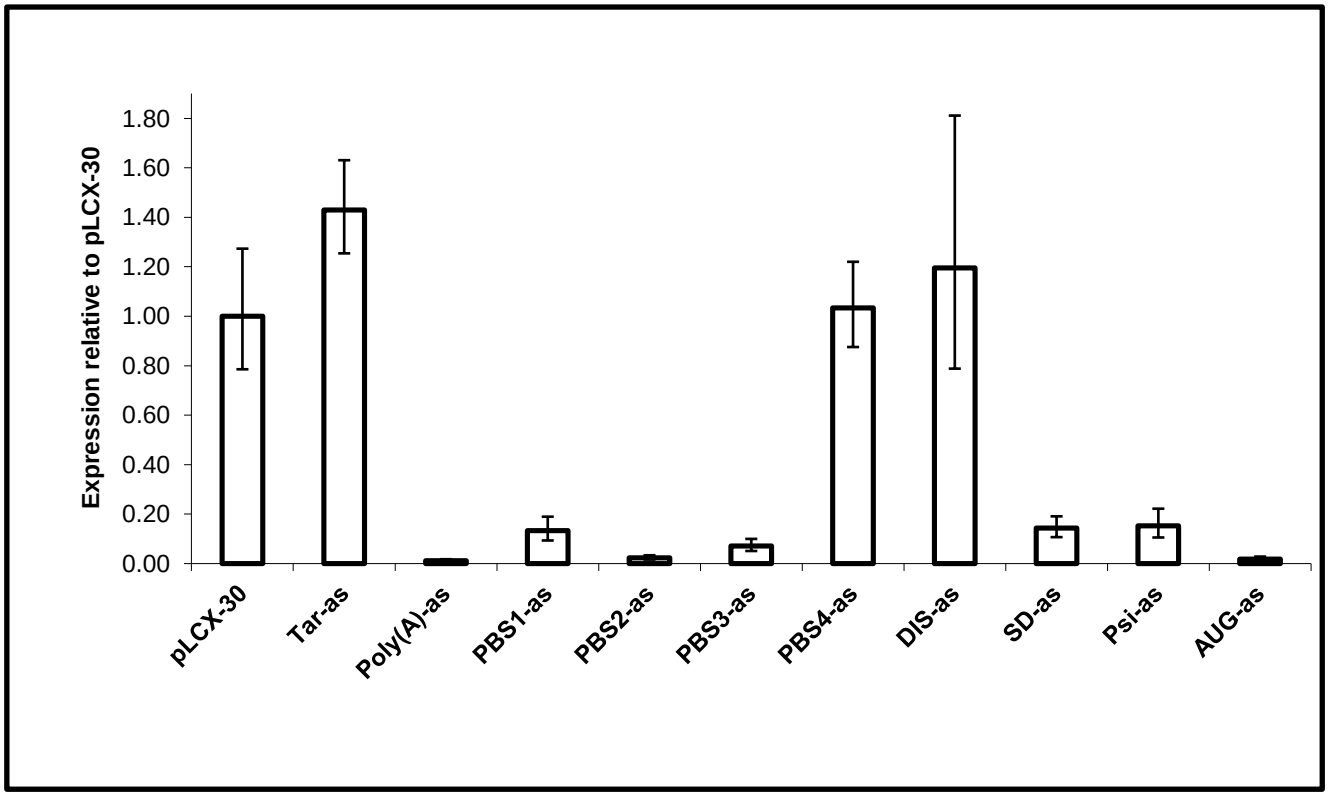
Expression relative to pLCX-30
1.80
1.60
1.40
1.20
1.00
0.80
0.60
0.40
0.20
0.00
pLCX-30
Tar-as
Poly(A)-as
PBS1-as
PBS2-as
PBS3-as
PBS4-as
DIS-as
SD-as
Psi-as
AUG-as